Fermi National Accelerator Laboratory

FN-363
1500.000

A Search for Chaotic Trajectories in Simulations of the Beam-Beam Interaction

D. Neuffer, A. Riddiford, A. Ruggiero

Fermilab, March 1982

Abstract

Results of a search for evidence of chaotic trajectories in simulations of beam storage with a "weak-strong" beam-beam interaction are presented. The storage ring tunes (ν_x, ν_y) and the beam-beam strength parameter $\Delta\nu$ are varied, and chaotic trajectories are found where the beam-beam spread $\Delta\nu$ contains low-order resonance intersections. Chaotic trajectories are not found if $\nu_x = \nu_y$. Variation of tune shift indicates that the degree of chaotic behavior does not directly depend on the tune spread but upon the relative location of the resonance intersection with respect to the tunes.

Operated by Universities Research Association Inc. under contract with the United States Department of Energy

I. Introduction

In a previous paper[1], we presented results which showed evidence for chaotic trajectories in a simulation of the beam-beam interaction with the parameters (ν_x=.245, ν_y=.12, $\Delta\nu$=.01), where ν_x, ν_y are the machine tunes and $\Delta\nu$ is the beam-beam tune shift. Other cases had not shown these chaotic trajectories. In another set of simulations[2], tune modulation was added to the beam-beam interaction, and it was found that chaotic trajectories could appear if the modulation amplitude wwere sufficiently large.

In this paper we change the parameter values (ν_x, ν_y, $\Delta\nu$) of the unmodulated two-dimensional beam-beam interaction and determine conditions for the appearance of chaotic trajectories, and the density of these chaotic regions.

II. Simulation Procedure

In our simulations we approximate particle circulation around the ring as the product of two transformations: a linear transport around the storage ring followed by a nonlinear beam-beam "kick" at the interaction area.

Transport around the ring can be represented by 2x2 matrices for both transverse (x and y) dimensions:

$$\begin{pmatrix} x \\ x' \end{pmatrix}_{After} = \begin{bmatrix} \cos 2\pi\nu_x & \beta_x \sin 2\pi\nu_x \\ -\dfrac{\sin 2\pi\nu_x}{\beta_x} & \cos 2\pi\nu_x \end{bmatrix} \begin{pmatrix} x \\ x' \end{pmatrix}_{Before} \tag{1}$$

In this linear transport x and y motion are decoupled. ν_x, ν_y, β_x, β_y are the usual Courant-Snyder tunes and beta-functions[3]. The beam-beam kick can be represented as

$$\begin{pmatrix} x \\ x' \end{pmatrix}_{After} = \begin{bmatrix} 1 & 0 \\ -\dfrac{4\pi\Delta\nu_x}{\beta_x} F_x(x,y) & 1 \end{bmatrix} \begin{pmatrix} x \\ x' \end{pmatrix}_{Before} \tag{2}$$

with a similar expression for y, y'.

The product of these transformations is equivalent to integration of the equation of motion:

$$x'' + K_x(s)\, x = -\frac{4\pi\Delta\nu_x}{\beta_x} F_x(x,y)\, x\, \delta_p(s) \tag{3}$$

s, the distance along the storage ring, is the independent variable, $\delta_p(s)$ is a periodic delta-function, and $K_{x,y}(s)$ is the focusing function.

In the present report we choose parameters which approximate the conditions[4] in: the Tevatron: $\beta_x^* = \beta_y^* = 2$ m, where the * indicates values matched to small amplitude motion, and we choose

$$F_x = F_y = \frac{1 - e^{-(x^2+y^2)/2\sigma^2}}{(x^2+y^2)/2\sigma^2} \tag{4}$$

with σ=0.0816 mm, which is the nonlinear force due to a round, gaussian charge distribution of rms radius σ.

Tune modulation can be added to the simulations by making ν_x, ν_y periodic in time[2]. In the present paper we choose <u>not</u> to do this and explore the properties of the variables ν_x, ν_y, $\Delta\nu$.

III. A Test for Chaotic Trajectories

In reference 1, we developed a useful empirical test for the appearance of chaotic trajectories; this is the repeatability test. In this test a particular trajectory is tracked forward for some large number of turns of the linear transformation and beam-beam kick and then the trajectory is reversed in time and tracked backward numerically (reversing the velocity) and forward and return positions are compared. A non-chaotic trajectory shows limited position error difference growths that is the error Δ increases with the number of turns N as $\Delta \sim \Delta_o N^{3/2}$ (or even as slowly as $\Delta_o N^{1/2}$ in some special cases[1]), where Δ_o is a single turn error magnitude ($\sim 10^{-26}$ double precision).

Chaotic trajectories develop substantially larger errors. Errors grow exponentially following

$$\Delta \sim \Delta_o \, e^{aN}$$

where a is a trajectory dependent parameter equal to the "Lyapunov Exponent" of nonlinear dynamics theory[5]. In nonlinear dynamics, "chaotic regions" are distinguished by the characteristic feature that nearby trajectories diverge from each other exponentially, with the rate of divergence given by the Lyapunov exponent.

In the repeatability tests of reference[1] particle trajectories fell quite naturally into one of two categories:

Category I: "repeatable" trajectories which develop errors of order 10^{-20} in a 100,000 turn reversability test and of order 10^{-15} after 100 million turns.

Category II: "chaotic" trajectories which exponentially develop errors of order unity after $\lesssim$100 thousand turns with measurable Lyapunov exponents of $\sim$.001.

Figures 1 and 2 show results of reversability tests for sample trajectories of both types. The clear empirical difference between them permits us to separate phase space into "chaotic" and "non-chaotic" regions.

In reference 1, for our case "B" (ν_x=.245, ν_y=.12, $\Delta\nu$=.01), it was found that 25% of a randomly selected sample of trajectories were chaotic. Other cases: (Case A: $\nu_x=\nu_y$=.245, $\Delta\nu$=.01) and (Case C: ν_x=.3439, ν_y=0.1772, $\Delta\nu$=.01) showed <u>no</u> chaotic trajectories. Empirical investigations indicate that chaotic trajectories can occur at the intersections of "low-order" resonances and do not occur when the tunes ν_x, ν_y are equal.

We want to point out that a chaotic trajectory is clearly associated

to a loss of "phase" memory, but we have no indication of amplitude growth. Actually we have evidence that for the period of time being simulated the chaotic trajectories remain confined to bounded domains in the phase space, with the exception possibly when tune oscillations are added[2].

IV. A Search in Tune Space (ν_x, ν_y) for Chaotic Trajectories

In this section, we report results of a more detailed search for chaotic trajectories. In this search, the tune shift $\Delta\nu$=.01 and the other parameters of the beam-beam interaction (the strong beam size and shape, and the matched betatron function of the weak beam $\beta_x^*=\beta_y^*=2m$) are kept constant while the tunes ν_x, ν_y are varied. These tunes are chosen near the intersections of low-order resonances; the intersections are at $\nu_x + \Delta\nu/2$, $\nu_y + \Delta\nu/2$ so that they are in the center of the beam-beam tune spread. A 100 sample trajectories are tracked forward 100,000 turns and returned, and their trajectories are inspected for chaotic behavior by the "repeatability test".

The initial coordinates (x, x', y, y') of these sample trajectories are randomly chosen within a 4-D phase volume weighted by a 4-D gaussian distribution determined by the parameters $\sigma^2=\sigma_x{}^2=\sigma_y{}^2$, and $\beta_x=\beta_y$, as defined above. Coordinate sets with an initial coordinate greater than three standard deviations are discarded. The same initial particle positions were used in all of the simulations, and particle motions are initiated at the center of the interaction region.

The results of 133 cases are displayed in Table 1, where accumulated errors between initial and return particle positions are tabulated. Trajectories separate naturally into two groups:

1. "non-chaotic" - with errors $\lesssim 10^{-19}$
2. "chaotic" - with errors of order unity; an error cut off of 10^{-10} is used to distinguish these.

There are a few with "intermediate" properties, with test errors between 10^{-10} and 10^{-19}. Most trajectories in this intermediate region are found to be "chaotic" with smaller Lyapunov exponents in a longer test. We therefore choose a boundary of 10^{-18} error to separate "chaotic" from "non-chaotic" regions.

The results show that chaotic trajectories do occur in many of the test cases. In the most "chaotic" case 31% of the test trajectories are chaotic.

A more careful analysis indicates that the cases with larger numbers of chaotic trajectories appear at the intersections of the lower order resonances. A resonance is determined by a relationship between the tunes:

$$n\,\nu_x + m\,\nu_y = p$$

where m, n, and p are integers. The "strength" of a nonlinear resonance is determined by the "order" Ω of the resonance which, for our round beam-beam force is given by

$$\Omega = |n| + |m| \qquad \text{if both m and n are even}$$

$$\Omega = 2\,(|n| + |m|) \qquad \text{if m and/or n are odd}$$

The appearance of only <u>even</u> orders is a result[7] of the fact that our beam-beam force is an even function of both x and y.

In our data set, which is confined to the tune region $0<\nu_x<1/2$, $0<\nu_y<1/2$ and avoids the diagonal $\nu_x=\nu_y$, in the present discussions the lowest order resonances are fourth order:

$$4\nu_x=1,\ 4\nu_y=1,\ 2\nu_x + 2\nu_y = 1$$

Sixth order resonances are:

$$3\nu_x=1,\ 6\nu_x=1,\ 3\nu_y=1,\ 6\nu_y=1$$
$$4\nu_x\pm2\nu_y=1,\ 4\nu_y\pm2\nu_x=1 \quad \nu_x\pm2\nu_y=1$$
$$2\nu_x\pm\nu_y=1 \quad \nu_x-2\nu_y=0 \quad \nu_y-2\nu_x=0$$

These resonances (4th and 6th order) are shown in Figure 3. Large numbers of chaotic trajectories ($\gtrsim$9%) appear in each intersection case tested. All cases with more than 7% chaotic are included within this set except for ν_x=.37, ν_y=.12 which is at the intersection of a fourth order and <u>five</u> eighth order resonances (14% chaotic).

Including eighth order resonances adds another set of intersections with fewer chaotic trajectories. Intersections of sixth , fourth or eighth with eighth order resonances have between 0% and 7% chaotic trajectories (with a single "fourth-eighth" case at 14% as noted above). Figure 4 shows these additional intersections. We note here that <u>all</u> cases (except 2) with more than 1 chaotic trajectory in our test cases are included within Figures 3 and 4. The exceptions are intersections of <u>fou</u>rth with tenth order resonances (3% and 2% chaotic).

In figure 5 we include higher order resonance intersections (up to twelfth). Most of the additional cases show <u>no</u> "chaotic" trajectories, although a few have a single "chaotic" case, with the two exceptions mentioned above.

We conclude this section with the summary that chaotic trajectories can appear with large density at the intersections of low order resonances, and that their density rapidly decreases with the increasing order of the resonances.

The evidence supports the empirical hypothesis that the volume of the chaotic region is proportional to the intersecting volumes of the resonant region. We believe that the chaotic regions are the same as the stochastic layers of many non-linear resonances[8].

V. Dependence of the density of chaotic trajectories on tune shift

We repeated some of the above test cases with $\Delta\nu$=.02 and $\Delta\nu$=.005. The tunes ν_x, ν_y were adjusted to keep the resonance intersection in the center of the spread. We find no dependence on tune shift.

Figures 6 and 7 display the 74 casees with $\Delta\nu$=.02 and the 75 cases with $\Delta\nu$=.005 used in this test, and they can be compared with the $\Delta\nu$=.01 cases of figures 3, 4, and 5. The differences are less than a strictly statistical random error pattern; this is related to the fact that the 100 initial particle positions are the same for all cases.

This result is in agreement with the hypothesis that the density of the chaotic region is related to the widths of the intersecting resonances[8]. It is a fact that for the beam-beam interaction, resonance width does not depend directly on tune shift to lowest order, but does depend on the relative location of the resonance with respect to the tune spread.

VI. Resonance "Intersections" with $\nu_x=\nu_y$

In the previous sections we omitted consideration of cases with $\nu_x=\nu_y$. We now report results of six such cases with ν=.12, .1617, .195, .245, .3283, .395 (1/8, 1/6, 1/5, 1/4, 1/3, and 2/5 resonances) and with $\Delta\nu$=.01 in all cases. No chaotic trajectories were observed.

This may seem somewhat unexpected since these cases contain low order resonances and might be expected to contain chaotic regions following the general discussion above. However, as has been proven[6], the case $\nu_x=\nu_y$ has intrinsically different dynamics from $\nu_x\neq\nu_y$. It has been proved that with $\nu_x=\nu_y$ and a round beam-beam force there exists an invariant of the motion, which in this case ($\beta_x=\beta_y$) is simply an angular momentum:

$$p_\theta = x'y - y'x$$

(The theorem of reference 6 is more general.)

This means that the dynamics of our $\nu_x=\nu_y$ cases contain one less degree of freedom and is therefore intrinsically one-dimensional (1-D) motion. This is intrinsically different from the 2-D motion with $\nu_x\neq\nu_y$. In particular the intersection of multidimensional resonances cannot occur in $\nu_x=\nu_y$ cases, only 1-D "single resonances" actually occur. Similarly an extensive search for chaotic trajectories in the 1-D case obtained from (1), (2), (3) and (4) with the truncation y=0 has been completely negative.

The above discussion and our observations confirm the hypothesis that the intersection of low-order 2-D resonances within the tune spread is necessary and sufficient condition for the appearance of chaotic trajectories.

VII. Chaotic Trajectories with $0<\nu_y<.5$, $.5<\nu_x<1.0$

In the above analysis we have only considered cases in the tune region $0<\nu_x<.5$, $0<\nu_y<0.5$. An obvious symmetry connects these cases with similar cases in $.5<\nu_x<1.0$, $.5<\nu_y<1.0$. The behavior in the quadrant $0<\nu_y<0.5$, $.5<\nu_x<1.0$ is less obvious so we have undertaken reversability tests at the crossings of fourth and sixth order resonances. The results are displayed in Figure 8, which can be compared with Figure 3.

An exact symmetry between the cases can be noted, indicating that the addition of 0.5 to one of the two tunes leaves the chaotic properties unchanged. In particular we note that the line $\nu_x=\nu_y+1/2$ $(2\nu_x-2\nu_y=1)$ contains no chaotic trajectories, which suggests that an invariant of motion exists in this case as in the $\nu_x=\nu_y$ case, providing 1-D motion. This case was not specifically covered in the theorem of reference 6.

References

1) D. Neuffer, A. Riddiford, and A. Ruggiero, FN-346, October 1981.

2) D. Neuffer, A. Riddiford, and A. Ruggiero, FN-359, February 1982.

3) E.D. Courant and H.S. Snyder, Annals of Physics 3 , 1 (1958).

4) The Fermilab Antiproton Source Design Report, February 1982.

5) Ya. G. Sinai, Introduction to Engodic Theory , Princeton University Press, 1976.

6) A.G. Ruggiero, Particle Accelerators, Vol. 12, No. 1, March 1982.

7) A.G. Ruggiero, FN-258, April 24, 1974, also Proceedings of the IXth Intern. Conf. on High Energy Accelerators, Stanford, CA, May 1974, page 419.

8) B.V. Chirikov, Physics Reports, Vol. 52 , No. 5, 1979, pages 263-379.

TABLE 1. Error profile for 117 intersections with $0 < \nu_x < 1/2$ and 16 intersections with $1/2 < \nu_x < 1$. $\Delta\nu = 0.01$ for all 133 intersections. For each intersection 100 particles were tracked 100,000 turns forward, storing (x,x',y,y') values every 1250 turns; then back to the starting turn zero, comparing (x,x',y,y') with forward values. The error calculated was $10^{-N} = \sqrt{(\Delta x)^2 + (\Delta y)^2 + (\beta_x \Delta x')^2 + (\beta_y \Delta y')^2}$ where Δx, $\Delta x'$, Δy, $\Delta y'$ were the differences between forward and reverse values. Calculations were done in double precision (the determinate of the transfer matrix C1*C4-C2*C3 $= 1 \pm \varepsilon$ where typical values of ε were $0.5E-28 < \varepsilon < 0.2E-27$); a particle was counted to have failed if $N < 18$. The decimal portion of N was dropped in order to compile the table below.

Lowest Order Lines	Intersection		Number Failed	N value <10	10	11	12	13	14	15	16	17	18	19	20	21	22	23	Failed particles
4 4	3/4,1/4	DIAGONAL $2\nu_x - 2\nu_y = 1$	0											11	61	25	2	1	
4 6	2/3,1/6		0											1	84	13	2		
	5/6,1/3		0											1	83	14	2		
	2/3,1/3	$\nu_x > 1/2$	26	25					$1^{(9)}$					4	54	15	1		4,7,8,(9),14,20,21,32,34,35,41,48,54,55,57,59,68,69,71,73,75,76,77,87,89,90
	2/3,1/4		11	9				$2^{(16,33)}$						7	57	22	3		1,(16),(33),34,37,41,44,47,54,57,95
	3/4,1/3		10	10										5	62	19	3	1	7,8,9,14,19,21,30,44,55,96
	3/4,3/8		19	19										2	58	18	2	1	1,2,7,8,14,19,21,30,33,34,37,41,44,50,54,55,77,94,96
	5/8,1/4		21	20							$1^{(35)}$		1	7	49	20	2		1,4,7,8,9,16,19,32,33,34,(35),37,41,44,47,54,57,71,76,95,96
	1/3,1/4		10	10										5	62	21	2		1,32,34,37,44,47,54,74,90,95
	1/3,1/6		30	28				$1^{(37)}$				$1^{(34)}$		2	49	18	1		4,7,8,9,14,20,22,30,31,(34),35,36,(37),41,48,54,55,57,59,68,69,71,73,75,76,77,87,89,90,95
	1/4,1/6		11	11										6	61	17	4	1	1,7,8,9,14,19,21,30,37,55,96

TABLE 1 (continued)

Lowest Order Lines	Inter-section	Number Failed	N value <10	10	11	12	13	14	15	16	17	18	19	20	21	22	23	Failed Particles
4 6	1/4,1/8	21	20								1(94)		2	75	17	2	1	1,2,8,9,14,19,21,30,33,34,35,36,37,44,54,55,61,75,77,(94),96
	3/8,1/4	21	19					1(7)		1(61)			6	54	17	1	1	2,4,(7),9,14,16,21,33,34,37,41,44,47,57,(61),71,74,80,90,95,96
6 6	2/3,5/12	10	10										1	68	16	5		1,2,14,19,21,34,54,57,90,95
	3/5,1/5	17	16				1(88)						2	68	12	1		1,4,7,9,19,21,32,34,37,47,55,61,71,77,(88),95,96
	3/5,3/10	12	12											71	16	1		1,7,9,14,19,30,32,54,55,71,95,96
	4/5,2/5	12	11						1(21)				1	72	13	2		1,4,9,14,19,(21),34,54,55,71,95,96
	5/6,5/12	7	7										1	72	17	3		1,9,14,19,21,34,55
	7/10,2/5	10	9							1(21)				75	14	1		1,2,9,14,19,(21),34,55,61,95
	7/12,1/3	8	7								1(75)		2	70	15	5		1,9,19,30,54,55,(75),96
	7/12,1/6	7	6			1(69)							1	73	16	3		7,14,19,21,34,37,(69)
	1/3,1/12	9	9										1	71	16	3		1,9,19,32,34,37,47,54,96
	1/5,1/10	12	10		1(1)				1(37)				1	71	14	2		(1),4,9,19,30,(37),54,55,61,71,95,96
	2/5,1/5	9	9										3	71	14	2	1	2,9,14,19,54,55,90,95,96
	2/5,3/10	11	10					1(90)					2	74	11	1	1	2,9,14,19,21,34,61,88,(90),95,96
	1/6,1/12	6	6										1	75	15	3		1,14,19,21,54,96
	3/10,1/10	16	15					1(95)				1	2	68	12	1		2,7,9,14,19,21,32,34,37,55,61,71,75,88,(95),96
	5/12,1/3	6	6											78	14	2		1,2,19,21,34,95
	5/12,1/6	7	6				1(55)					1	2	72	16	2		9,14,21,30,34,(55),61

$\gamma_x > 1/2$

TABLE 1 (continued)

Lowest Order Lines	Inter-section	Number Failed	N value <10	10	11	12	13	14	15	16	17	18	19	20	21	22	23	Failed Particles
4 8	1/4,1/12	5	5										5	70	17	2	1	8,9,19,30,96
	3/8,1/8	14	12				1(89)				1(69)		1	67	17	1		4,20,30,36,41,47,54,68,(69),75,77,87,(89),90
	5/12,1/4	5	5									1	4	68	20	2		37,54,88,90,95
6 8	1/3,1/8	2	2										1	76	18	3		14,21
	1/3,1/9	3	2							1(1)				79	15	3		(1),14,19
	1/3,2/9	2	2											76	19	3		14,19
	1/3,1/18	3	3											79	15	3		1,14,21
	1/3,5/18	2	2											82	13	3		14,19
	1/6,1/8	2	1	1(21)									1	77	16	4		14,(21)
	1/6,1/9	5	5										1	76	15	3		1,14,19,21,34
	1/6,1/18	1	1										1	79	16	3		14
	1/7,1/14	1	1											83	15	1		21
	2/7,1/7	2	2										2	84	11	1		14,96
	2/7,1/14	4	4											84	11	1		9,14,21,34
	3/7,1/7	1	1											79	18	2		96
	3/7,2/7	5	4								1(2)			78	15	2		(2),9,14,19,61
	3/7,3/14	4	3			1(34)								80	14	2		1,61,95
	3/7,5/14	6	6									1		79	13	1		1,9,14,19,34,55
	1/8,1/16	2	2											80	16	2		4,21
	3/8,1/3	0											1	83	12	3	1	
	3/8,1/6	1	1										2	80	14	2	1	1
	3/8,1/16	2	2										1	80	15	1	1	2,88
	3/8,3/16	0												87	11	1	1	
	3/8,5/16	2	2										1	79	16	1	1	34,95

TABLE 1 (continued)

Lowest Order Lines	Inter-section	Number Failed	N value <10	10	11	12	13	14	15	16	17	18	19	20	21	22	23	Failed particles
6 8	2/9,1/6	3	3									1	2	80	12	2		14,19,21
	4/9,1/3	2	1			1(95)								77	19	2		1,(95)
	4/9,1/6	3	3										2	74	18	3		1,21,34
	3/14,1/7	3	3									1	7	75	13	1		14,61,96
	3/14,1/14	1		1(4)										80	17	2		(4)
	5/14,2/7	4	3						1(9)				1	80	12	3		(9),54,61,96
	5/14,1/14	2	1						1(9)				1	80	16	1		(9),61
	5/14,3/14	7	7										1	81	10	1		9,14,19,21,34,55,61
	3/16,1/8	2	1			1(61)							1	80	16	1		30,(61)
	5/16,1/8	2	2											85	12	1		21,34
	7/16,1/8	0											1	78	19	2		
	7/16,3/8	2	1		1(34)									82	15	1		19,(34)
	5/18,1/6	1							1(14)				2	82	13	2		(14)
	7/18,1/3	2	2											79	17	2		1,21
	7/18,1/6	0											2	78	18	2		
8 8	1/8,1/24	0											1	80	17	2		
	3/8,1/24	1	1											85	12	1	1	21
	3/8,5/24	0											1	86	11	1	1	
	3/8,7/24	0												88	10	1	1	
	3/16,1/16	3	3										1	85	10	1		14,21,96
	5/16,1/16	2	2											85	12	1		14,21
	7/16,3/16	3	3											81	14	2		1,19,34
	7/16,5/16	3	3											80	16	1		1,21,34
	3/20,1/20	0											2	86	11	1		
	7/20,1/20	1	1										1	86	11	1		21

TABLE 1 (continued)

Lowest Order Lines	Inter-section	Number Failed	N value <10	10	11	12	13	14	15	16	17	18	19	20	21	22	23	Failed particles
8 8	9/20,3/20	0												82	15	3		
	9/20,7/20	2	2										1	82	13	2		1,61
	5/24,1/8	1	1											87	11	1		21
	7/24,1/8	2	1						1(14)					86	11	1		(14),21
	11/24,1/8	1						1(90)						83	14	2		(90)
	11/24,3/8	0												84	15	1		
4 10	1/4,1/5	0											4	76	17	2	1	
(8 out of 10)	1/4,1/16	3	3										5	70	19	2	1	9,19,96
	1/4,3/16	1	1										4	75	17	2	1	55
	2/5,1/4	0											6	79	13	1	1	
	2/5,1/10	0										1	5	74	19	1		
	3/10,1/5	0											9	73	17	1		
	5/16,1/4	2	2										4	75	18	1		54,74
	7/16,1/4	1						1(90)					4	72	22	1		(90)
4 12	5/12,1/12	0										1	1	79	18	1		
6 10	1/3,1/5	0												82	16	2		
(8 out of 36)	2/5,1/3	0												85	12	2	1	
	2/9,1/9	0												88	11	1		
	4/9,1/9	0											1	77	21	1		
	4/9,2/9	0												85	14	1		
	5/18,1/18	1	1											86	12	1		21
	7/18,1/18	0												81	18	1		
	7/18,5/18	1						1(9)					1	84	13	1		(9)

TABLE 1 (concluded)

Lowest Order Lines	Inter-section	Number Failed	N value <10	10	...	17	18	19	20	21	22	23	Failed Particles
8 10	1/5,1/15	0							89	10	1		
(19 out of 96)	1/5,1/20	0							88	11	1		
	2/5,2/15	0						2	86	10	1	1	
	2/5,3/20	0						1	86	11	1	1	
	2/5,7/20	0						2	84	12	1	1	
	3/11,1/11	1	1						88	10	1		21
	3/11,2/11	1	1						88	10	1		14
	4/11,1/11	0							86	13	1		
	5/11,2/11	1	1					1	82	14	2		1
	5/11,4/11	0						1	84	14	1		
	3/13,1/13	1				1(21)			88	10	1		(21)
	4/13,1/13	0							89	10	1		
	4/13,3/13	0						2	86	11	1		
	5/13,2/13	0						1	84	14	1		
	6/13,2/13	0							85	13	1	1	
	6/13,5/13	0							85	14	1		
	4/15,1/5	0							89	10	1		
	7/15,2/5	0							87	12	1		
	9/20,1/5	1		1(1)					84	14	1		(1)
10 10	1/5,2/15	0							89	10	1		
(13 out Of 80)	2/5,1/15	0							87	11	1	1	
	2/5,4/15	0							88	10	1	1	
	3/13,2/13	0							87	12	1		
	5/13,1/13	0						1	84	14	1		
	6/13,4/13	0							86	13	1		
	4/15,1/15	0							88	11	1		
	7/15,1/5	0							87	12	1		
	7/15,2/15	0							87	12	1		
	4/17,1/17	0						1	87	11	1		
	5/17,3/17	0							89	10	1		
	7/17,6/17	0							87	12	1		
	8/17,2/17	0							87	12	1		

Figure 1. Repeatability errors; Case B: $\nu_x = 0.245$; $\nu_y = 0.120$; $\Delta\nu = 0.010$

Initial Conditions: $X'_o = Y'_o = 0$

$X_o = Y_o = A\sigma$, where $A = 0.5$, 1.0 and 2.0; $\sigma = 0.08165$ mm

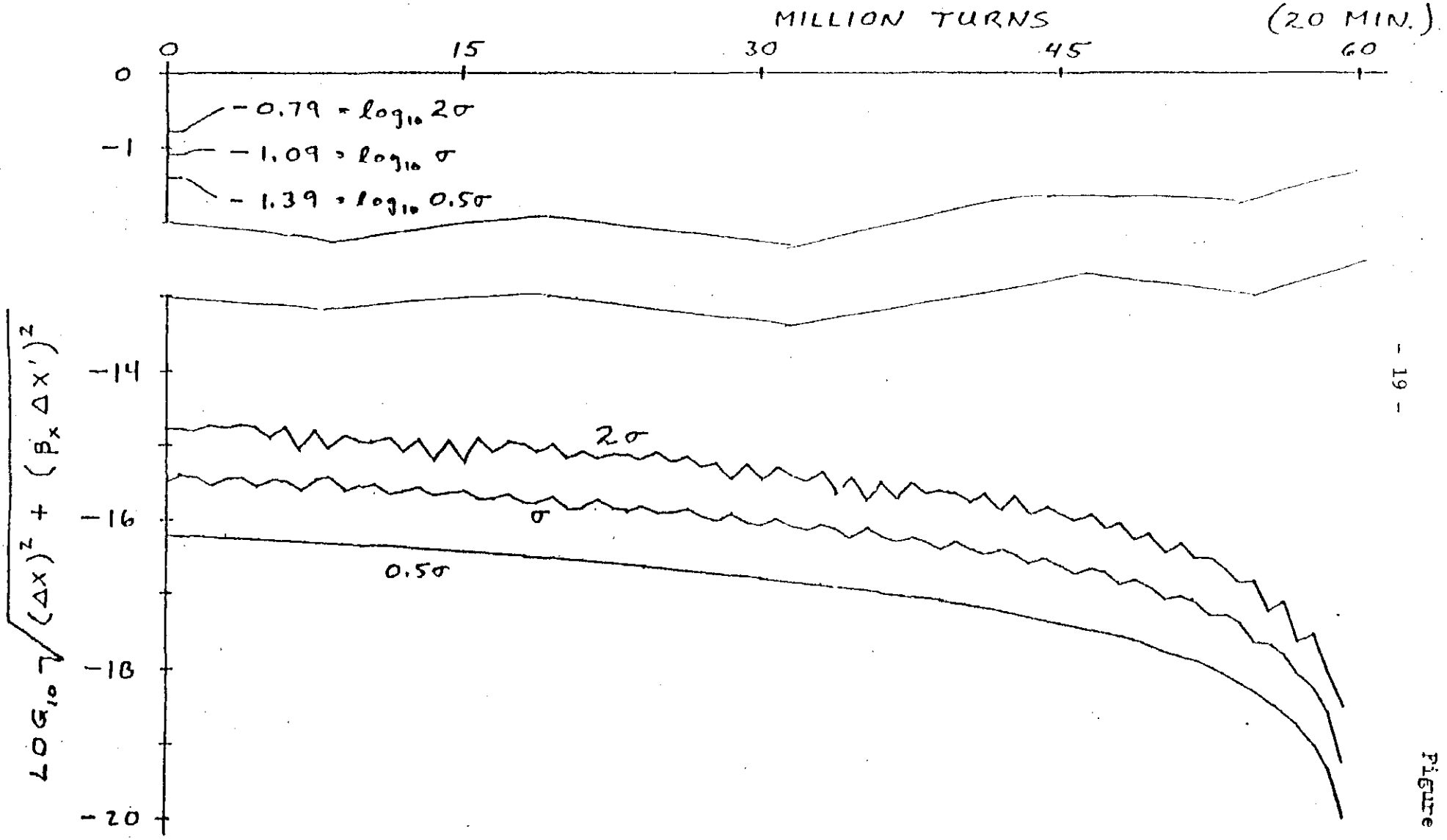

Figure 1

Figure 2. Repeatability errors; Case B: $\nu_x = 0.245$; $\nu_y = 0.120$; $\Delta\nu = 0.010$
Initial Conditions: $X_o = Y_o = 1.5\sigma = 0.1225$ mm; $X'_o = Y'_o = 0$

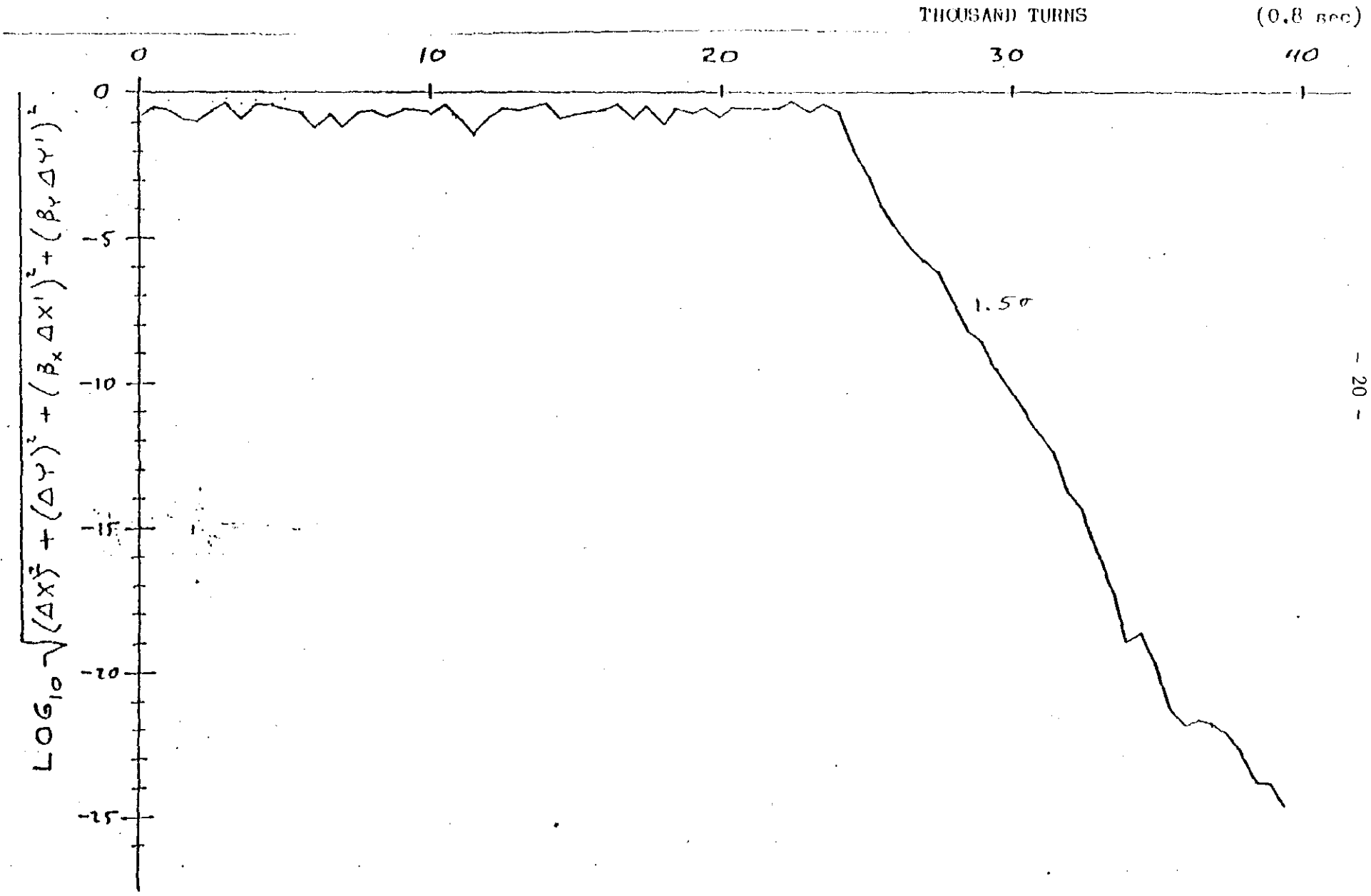

Figure 2

Figure 3

Tune space showing all lines of order 4 and 6, and the number of chaotic trajectories (out of 100) at the 13 intersections; 5 are between lines whose lowest orders are 4 and 6; 8 are between lines whose lowest orders are 6 and 6. The 4th order lines are darkened.

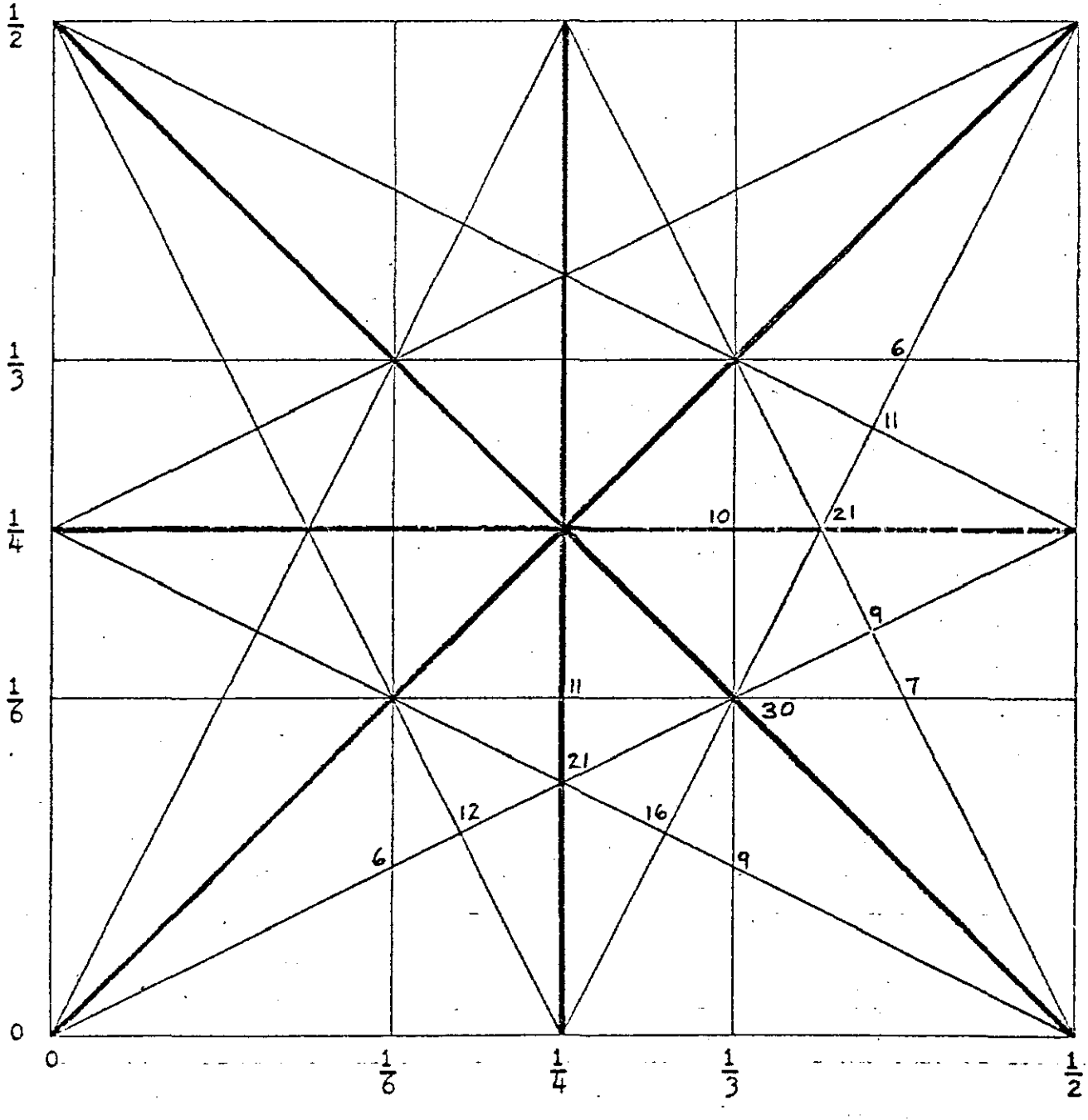

Tune space showing all lines of orders 4, 6 and 8, and the number of chaotic trajectories (out of 100) at the 55 intersections between 8th order lines and 4th order (3), 6th order (36) and 8th order (16) lines.

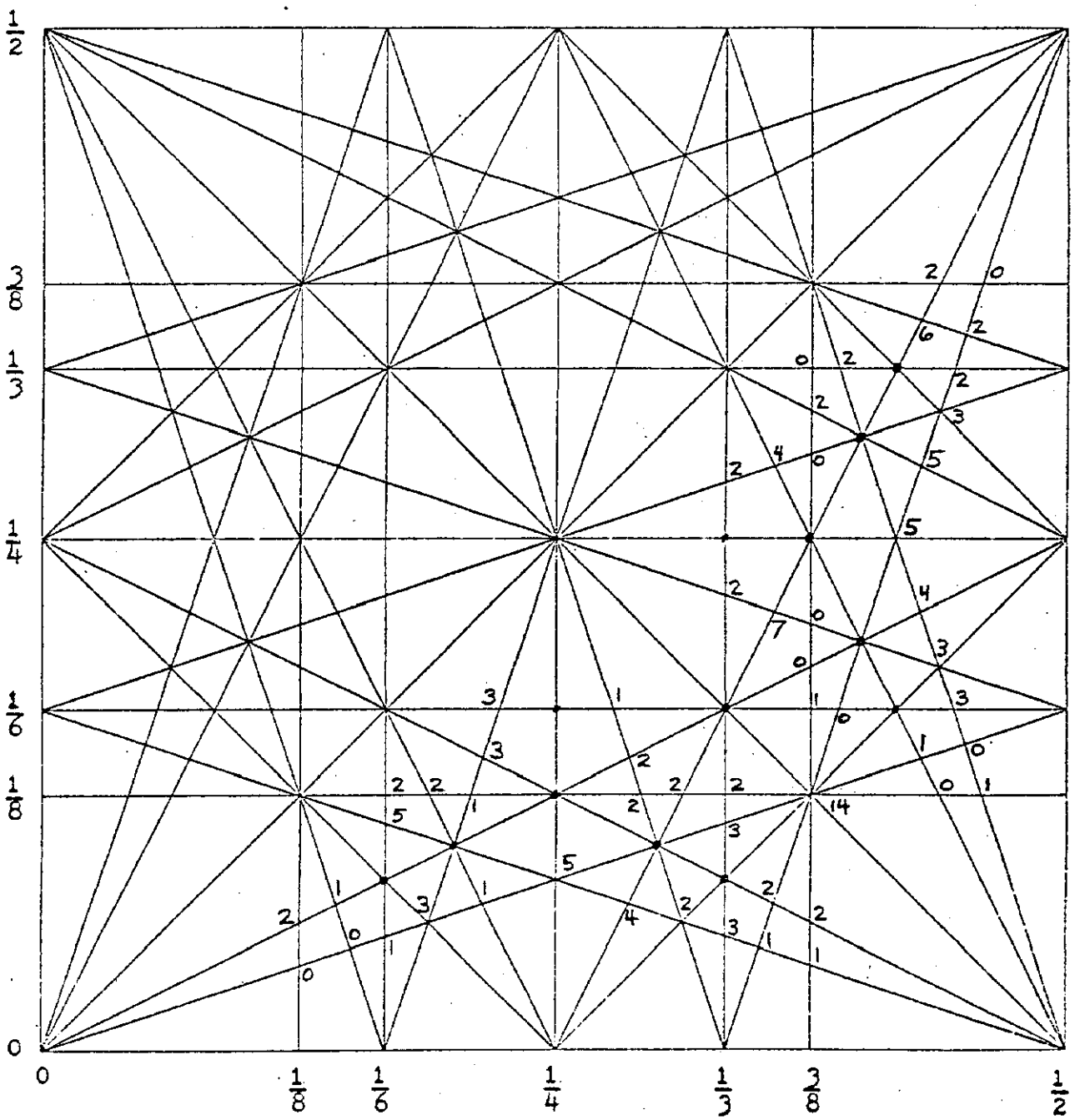

Figure 5

Tune space showing all lines of orders 4, 6, 8, and 10, and the number of chaotic trajectories (out of 100) at 49 intersections between 10th order lines and 4th order (8), 6th order (8), 8th order (19), 10th order (13); and one intersection between a 4th order line and a 12th order line sketched in.

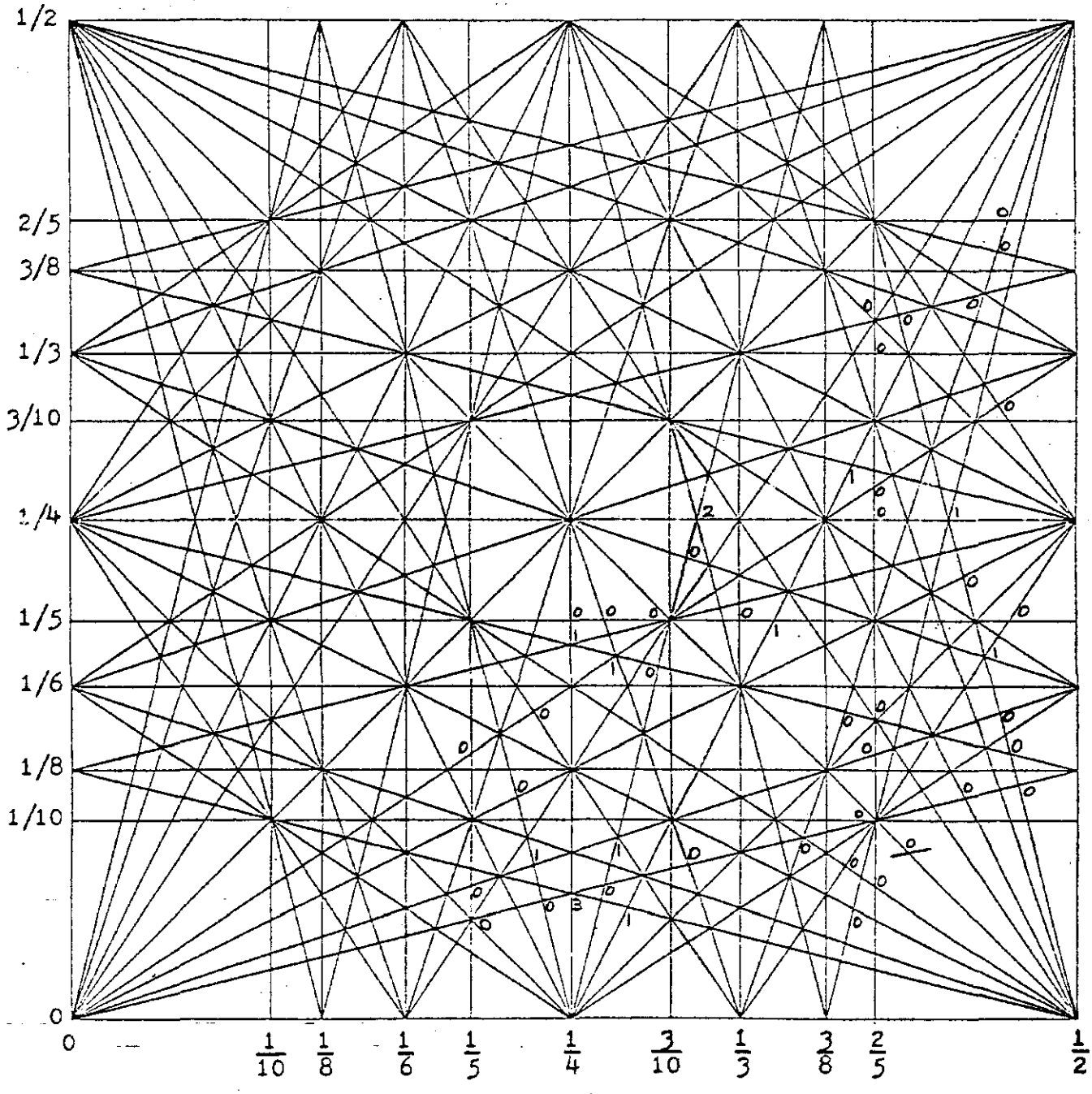

Figure 6 Tune space showing all lines of order 6 or less, and the number of non-reversible particles at 74 intersections for $\Delta\nu = 0.02$

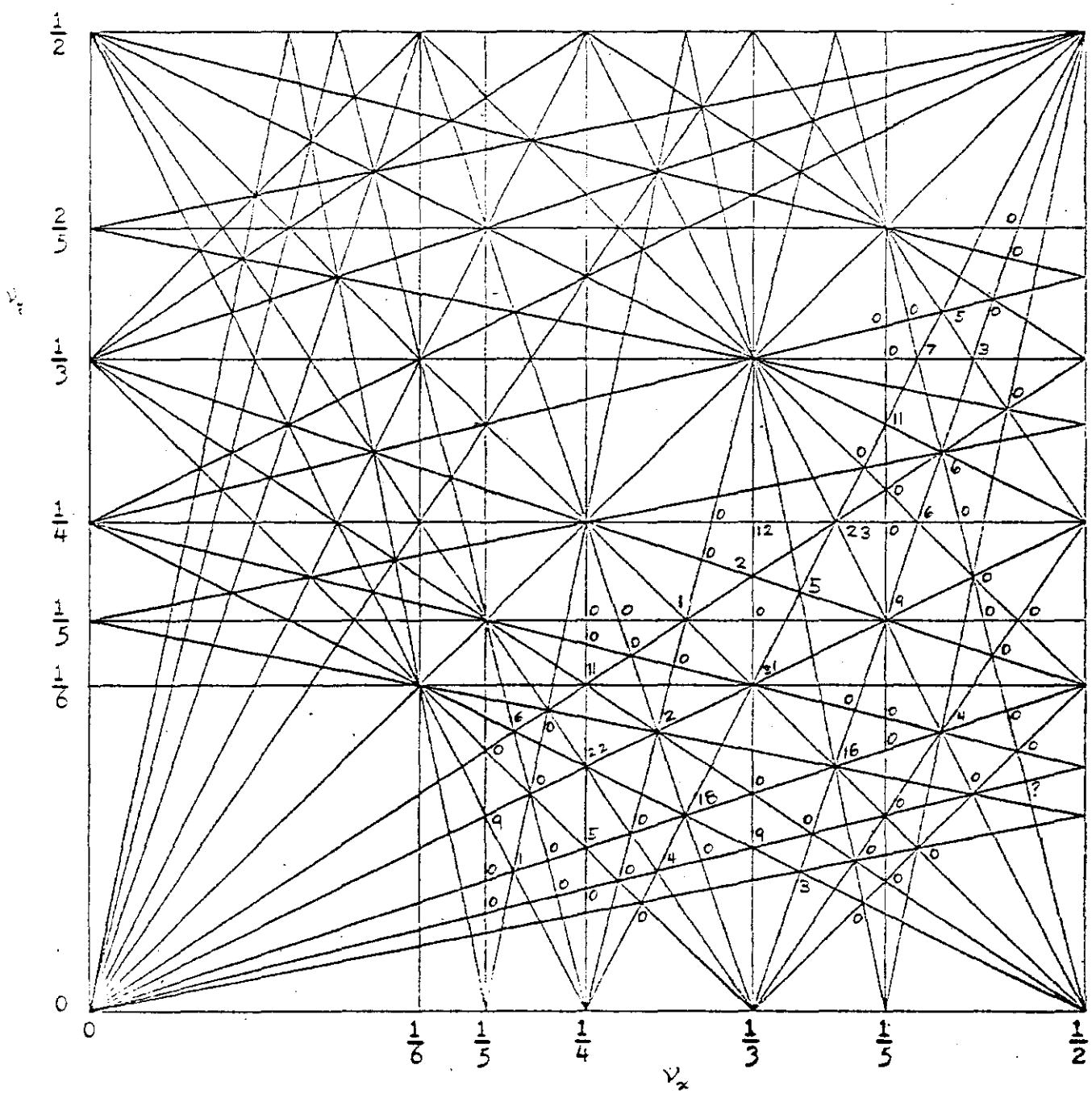

Figure 7 Tune space showing all lines of order 6 or less, and the number of non-reversible particles at 75 intersections for $\Delta\nu = 0.005$

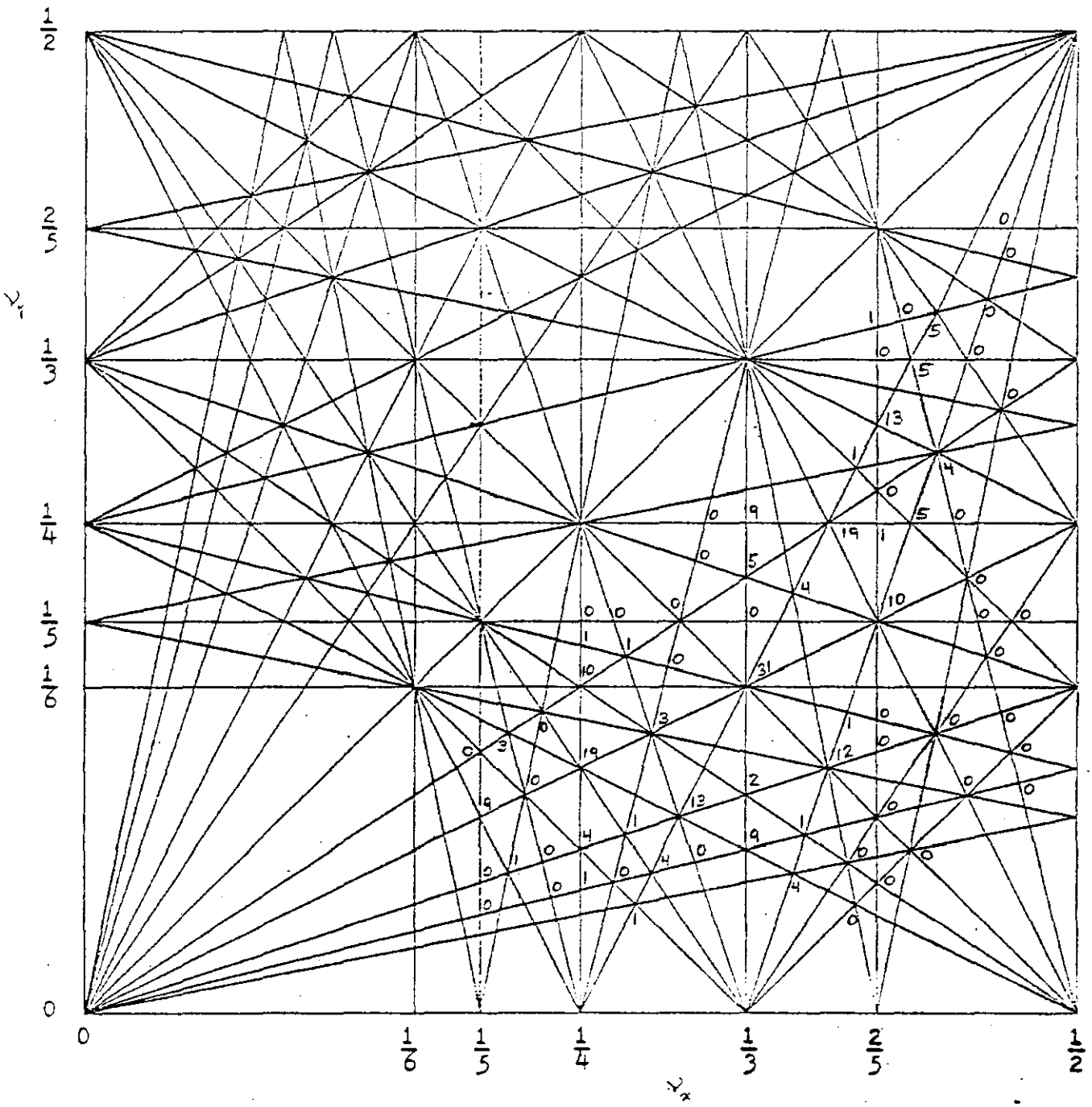
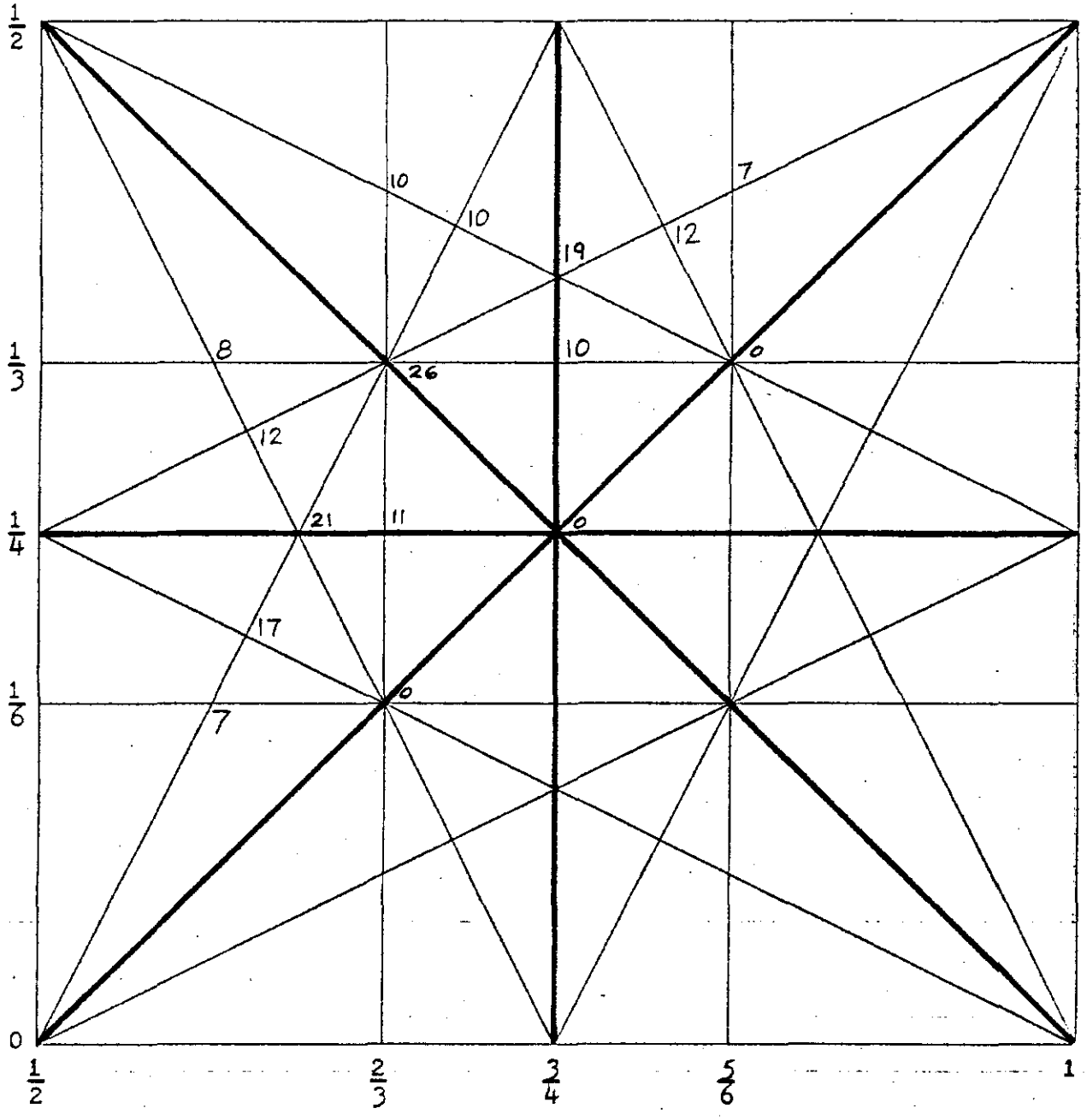
Tune space for $1/2 < \nu_x < 1$ showing all lines of order 4 (darkened) and 6; and the number of chaotic trajectories (out of 100) at 16 intersections: one is between lines whose lowest orders are 4 and 4; 7 are between lines whose lowest orders are 4 and 6; 8 are between lines whose lowest orders are 6 and 6.